HHS Public Access

Author manuscript

Mol Cancer Ther. Author manuscript; available in PMC 2016 April 01.

Published in final edited form as:

Mol Cancer Ther. 2015 April ; 14(4): 1035–1047. doi:10.1158/1535-7163.MCT-14-0800.

Targeted blockade of JAK/STAT3 signaling inhibits ovarian carcinoma growth

Galina Gritsina[1], **Fang Xiao**[1], **Shane W. O'Brien**[1], **Rashid Gabbasov**[1,†], **Marisa A. Maglaty**[1], **Ren-Huan Xu**[2], **Roshan J. Thapa**[2], **Yan Zhou**[3], **Emmanuelle Nicolas**[4], **Samuel Litwin**[3], **Siddharth Balachandran**[2], **Luis J. Sigal**[2], **Dennis Huszar**[5], and **Denise C. Connolly**[1]

[1]Molecular Therapeutics Program

[2]Immune Cell Development and Host Defense Program

[3]Biostatistics Facility

[4]Genomics Facility, Fox Chase Cancer Center, Philadelphia, PA, USA

[5]AstraZeneca Oncology iMed, Waltham, MA, USA

[†]Kazan (Volga region) Federal University, Kazan, Russia

Abstract

Ovarian carcinoma (OC) is the fifth leading cause of death among women in the United States. Persistent activation of signal transducer and activator of transcription (STAT3) is frequently detected in OC. STAT3 is activated by Janus family kinases (JAK) via cytokine receptors, growth factor receptor and non-growth factor receptor tyrosine kinases. Activation of STAT3 mediates tumor cell proliferation, survival, motility, invasion, and angiogenesis, and recent work demonstrates that STAT3 activation suppresses anti-tumor immune responses and supports tumor-promoting inflammation. We hypothesized that therapeutic targeting of the JAK/STAT3 pathway would inhibit tumor growth by direct effects on OC cells and by inhibition of cells in the tumor microenvironment (TME). To test this, we evaluated the effects of a small molecule JAK inhibitor, AZD1480, on cell viability, apoptosis, proliferation, migration and adhesion of OC cells *in vitro*. We then evaluated the effects of AZD1480 on *in vivo* tumor growth and progression, gene expression, tumor-associated matrix metalloproteinase (MMP) activity and immune cell populations in a transgenic mouse model of OC. AZD1480-treatment inhibited STAT3 phosphorylation and DNA binding, and migration and adhesion of cultured OC cells and ovarian tumor growth rate, volume and ascites production in mice. In addition, drug treatment led to altered gene expression, decreased tumor-associated MMP activity, and fewer suppressor T cells in the peritoneal tumor microenvironment of tumor-bearing mice than control mice. Taken together, our results show pharmacological inhibition of the JAK2/STAT3 pathway leads to disruption of functions essential for ovarian tumor growth and progression and represents a promising therapeutic strategy.

Corresponding author: Denise C. Connolly, Molecular Therapeutics Program, 333 Cottman Ave., W310, Philadelphia, PA 19111, Phone: 215-728-1004, FAX: 215-728-2741, Denise.Connolly@fccc.edu.

Conflicts of interest: Dennis Huszar is an employee of AstraZeneca. The remaining authors have no conflicts of interest to declare.

Keywords

JAK; STAT3; ovarian cancer; AZD1480

Introduction

Ovarian carcinoma (OC) is the leading cause of morbidity and mortality among gynecological cancers, with over 21000 new cases and 14270 deaths estimated in the United States in 2014 (1). Early stage ovarian cancer presents with few if any symptoms which results in delayed diagnosis by which time the disease has spread beyond the ovary and is at late stage (Stage III or IV). The standard treatment for women diagnosed with OC is aggressive surgical debulking accompanied by cytotoxic chemotherapy consisting of carboplatin and paclitaxel. Disease that initially responds well to this treatment frequently relapses in a more aggressive form and in most cases becomes drug-resistant. With the exception of anti-angiogenic VEGF-targeted therapeutics or PARP inhibitors, few targeted therapies have shown efficacy, and drug-resistant recurrent ovarian cancer remains incurable. One of the reasons for the lack of success in identifying effective targeted agents is that OCs are a group of cancers that differ in histology, genetic alterations and cellular signaling pathway activation. High grade serous carcinomas (HGSC) are the most common, aggressive and lethal subtype of OC. Extensive genomic analyses showed that nearly all HGSC have p53 mutations, but few common drug-targetable alterations (2). These cancers exhibit significant genetic instability and tumor heterogeneity, and lack common actionable oncogenic driver mutations. Therefore, in order for targeted therapies to show efficacy, they will likely need to have wide ranging biological effects (3).

An attractive therapeutic target, based on its common activation in OC and its broad cellular activities, is signal transducer and activator of transcription 3 (STAT3). STAT3 is a cytoplasmic transcription factor that mediates cytokine and growth factor signaling upon activation by Janus family kinases (JAKs), receptor tyrosine kinases and non-receptor tyrosine kinases associated with cytokine receptors (4). In normal tissues STAT3 activation is strictly controlled, but the phosphorylated activated form of STAT3 is constitutively expressed in over 70% of solid and hematological tumors (5-7). STAT3 activation contributes to tumorigenesis via multiple cellular functions and biological processes, including proliferation, survival, angiogenesis, metastasis, inflammation and immune evasion (8). Several studies have shown that STAT3 is constitutively activated in OC cell lines and primary human tumors (7, 9, 10). Activation of STAT3 is more commonly correlated with clinically aggressive high grade OC than more indolent low grade cancers (7). High levels of expression of IL-6 are common in OC cells, ascites and patient sera, supporting prominent activation of an IL-6/JAK/STAT3 signaling axis in OC cells and the tumor microenvironment (11, 12). Moreover, a number of recent studies show that STAT3 activation in inflammatory cells in the tumor microenvironment directly supports tumor initiation and maintenance in some cancers (13-15).

The dual role of persistent STAT3 activation in tumor-promotion through tumor-intrinsic and tumor-extrinsic contributions in the tumor microenvironment (6, 16, 17) suggests that

targeted inhibition of this signaling pathway would be a promising therapeutic approach for OC. However, direct therapeutic targeting of STAT3 is somewhat challenging due to the lack of drug-targetable intrinsic catalytic activity of the protein. Natural products, small molecule and decoy oligonucleotide inhibitors have been developed (reviewed in (18)), with decoy oligonucelotides in early clinical development (19). An alternative, clinically relevant, and currently available strategy is inhibition of upstream STAT3 activators, by targeted blockade of JAKs (16, 20).

The therapeutic potential of targeting the JAK2/STAT3 pathway with AZD1480, a small molecule ATP-binding inhibitor of JAK1/2 (16), has been investigated in models of several non-ovarian solid tumors, including glioblastoma, breast, small cell lung, prostate and gastrointestinal cancers (6, 20-25). Based on the importance of the IL-6/JAK/STAT3 signaling axis in OC, we sought to explore the therapeutic effects of AZD1480 in the context of OC, using human OC cell lines and a transgenic mouse model that develops spontaneous OC similar to human HGSC with 100% penetrance (26, 27). Employment of an immunocompetent genetically engineered mouse (GEM) model of OC enabled the analysis of AZD1480-mediated effects on primary tumor growth and on the immune and tumor microenvironment. In this study, we show that targeted blockade of the JAK/STAT3 pathway inhibited ascites production, tumor-associated protease activity, pro-tumorigenic cancer-associated inflammatory mediators and OC growth *in vivo*. These observations identify the JAK/STAT3 pathway as a potential therapeutic target in OC.

Materials and Methods

Cell lines, culture conditions and reagents

The cell lines employed in this study were chosen based on high levels of phosphorylated, constitutively activated STAT3 as detected by pSTAT3^{Y705} ((3) and Xiao and Connolly, unpublished data). Human ovarian carcinoma cell (OC) lines OVCAR-5, OVCAR-8 and A1847 were obtained from the Fox Chase Cancer Center (FCCC) Cell Culture Facility (deposited by Dr. Thomas Hamilton). The identity of the cells was authenticated by short tandem repeat (STR) analysis and comparison to early passage stocks of the parental cells donated by Dr. Hamilton. Human OC cells were cultured in RPMI-1640 media (Life Technologies) supplemented with 10% fetal bovine serum (Atlanta Biologicals), penicillin/streptomycin (100 units/mL and 100 μg/mL respectively, Life Technologies/Invitrogen), 0.25 units/ml insulin (Novo Nordisk). MOVCAR-5009 and MOVCAR-5447 were derived in our laboratory from the ascites of ovarian tumor bearing female *TgMISIIR-TAg* (27). MOVCAR-5009 cells stably transduced with retroviral STAT3 targeting shRNA or shMLP vector (28), were cultured in DMEM media supplemented with 4% FBS, penicillin/streptomycin, and 1× insulin/transferrin/selenium (supplied as a 100× stock by Life Technologies/Invitrogen). The structure of AZD1480 is published (16) and drug was provided by AstraZeneca (Waltham MA; D.H.) and dissolved in DMSO (Sigma) for in vitro experiments. For *in vivo* drug dosing, AZD1480 was formulated in 0.5% hypermellose/0.1%Tween 80 (Sigma). Recombinant human IL-6 (PeproTech), 25 ng/ml, was administered to cells for 3 hours. Primary antibodies used were: α-pJAK2$^{Y1007/1008}$, α-pSTAT3^{Y705}, α-

STAT3 and α-JAK2 (all from Cell Signaling Technology); α-β actin and α-TAg (Santa Cruz Biotechnology); α-cleaved $PARP^{214/215}$ (Millipore).

Cell viability, proliferation and apoptosis assays

The effects of AZD1480 on OC cell viability were evaluated using CellTiter-Blue® Cell Viability Assay (Promega) according to manufacturer's instructions. Cells (3×10^4 cells/ml) were plated in triplicate on 96-well plate, allowed to adhere for 24 hours then treated with AZD1480 (0 – 10 μmol/L) for 72 hours prior to analysis. To evaluate the effect of drug treatment on proliferation 1.7×10^4 cells were plated in 24-wells plates, incubated for 24 hours, then treated with AZD1480 (0 – 10 μmol/L). After 6-72 hours of drug treatment, plates were fixed in 4% paraformaldehyde, stained with 0.1% crystal violet and absorbance measured at 590 nm. Induction of apoptosis was evaluated by Annexin V staining (Guava Nexin Reagent, Millipore) of cells treated with 0 – 5 μmol/L AZD1480 for 48 hours. Cells were harvested, washed, incubated with Guava Nexin staining solution and measured using the Guava EasyCyte system and accompanying Cytosoft 3.6.1 software (Merck Millipore). 100nM Etoposide (Sigma-Aldrich) was used as a positive control for induction of apoptosis.

Migration and adhesion assays

Migration was assayed and quantified as described (29). Briefly, 4×10^4 cells were suspended in serum free media and seeded in duplicate in 24-well cell culture plates containing 8 μm pore inserts. Complete media was added to the bottom chamber and the plate was incubated for 24 hours at 37°C in 5%CO_2. Cells were fixed with 4% paraformaldehyde, stained with 1% crystal violet in 25% methanol and five bright-field images per insert (10 × magnification) were taken with a CCD camera coupled to a Nikon Eclipse E800 microscope. Cellular adhesion was assayed by suspending cells in serum free media and plating in triplicate on 96-well plates pre-coated with 10 μg/ml type I collagen (BD BioSciences), 2 μg/ml fibronectin (Sigma Aldrich) or 3% bovine serum albumin (control). After 1 hour incubation, adherent cells were fixed with 4% PFA, stained with crystal violet and counted. Migration and adhesion experiments were repeated three times and the mean number of cells/field (migration) or mean number of cells/well ± SEM calculated.

Immunoblot and ELISA analysis

Cells and tissue were lysed with Mammalian Protein Extraction Reagent (MPER) or Tissue Protein Extraction Reagent (TPER), respectively (Thermo Scientific). Lysis buffers were supplemented with Halt Phosphatase Inhibitor Cocktail (Thermo Scientific) and Complete Mini Protease Inhibitor Cocktail (Roche Diagnostics), and protein concentration was determined using the BCA (bicinchoninic acid) assay (Thermo Scientific). Immunoblotting was performed as described (3, 29): Protein extracts were subjected to SDS-PAGE on 4-12% gradient polyacrylamide gels (Life Technologies) and transferred to PVDF membrane (Millipore). Membranes were blocked in 5% non-fat milk in PBST, incubated overnight at 4°C with primary antibody, followed by horseradish conjugated secondary antibody (GE Healthcare, Pittsburgh, PA, USA) and signal detected with SuperSignal West Pico Chemiluminescent Substrate (Thermo Scientific). To determine the effects of AZD1480 treatment on STAT3 activation, vehicle- and drug-treated tumors were lysed in

cold TPER containing protease and phosphatase inhibitors, homogenized in a Precellys Homogenizer (vendor) and pSTAT3^{Y705} determined by immunoblot analysis with α-pSTAT3^{Y705} antibodies and by electrochemiluminescent ELISA pSTAT3^{Y705} assay (MesoScale Discovery) according to manufacturer's instructions.

Electrophoretic molecular shift assay (EMSA)

The effects of AZD1480 treatment on STAT3 DNA binding activity was performed by EMSA analysis as described (30). Briefly, cells were grown the presence or absence of AZD1480 (concentration) for 24 hours, and nuclear extracts prepared by lysis at 4C° in buffer containing 10 mmol/L HEPES, 10 mmol/L KCl, 1.5 mmol/L $MgCl_2$ and 1 mmol/L dithiothreitol (DTT) supplemented with protease and phosphatase inhibitors (as described for immunoblotting analysis) followed by addition of 10% IGEPAL CA-630 (octylphenoxypolyethoxyethanol). Nuclei were isolated by centrifugation and resuspended in nuclear lysis buffer containing 20 mmol/L HEPES, 400 mmol/L NaCl, 1.5 mmol/L $MgCl_2$, 0.2 mmol/L EDTA, 1 mmol/L DTT and 5% glycerol, and supplemented with protease and phosphatase inhibitors. MOVCAR-5009 cells stably transduced with a STAT3 targeted shRNA was used as a negative control for DNA binding and cells treated for 3 hours with 25 ng/ml recombinant IL-6 were used as a positive control. Protein concentration was determined with Bradford assay (Bio-Rad). Nuclear extracts were incubated with [^{32}P]-conjugated oligonucleotide probe containing STAT3 consensus-binding sequence (5′-AGC TTC ATT TCC CGT AAA TCC C-3′; Invitrogen) or a mutant oligonucleotide (5′-GAT CCT TCT GGG CCG TCC TAG ATC-3′; Santa Cruz Biotechnology). DNA binding specificity was determined by supershifting DNA-STAT3 complexes following pre-incubation of samples with an α-STAT3 antibody. Samples were subjected to 5% non-denaturing PAGE and gels were vacuum dried and exposed to radiography film.

Transgenic mice and drug treatment

All procedures involving mice were approved by the FCCC Institutional Animal Care and Use Committee (IACUC). C57BL/6J*TgMISIIR-TAg* mice have been described (26) and are maintained under pathogen free conditions on a standard rodent diet (2018SX Teklad Global, Harlan Laboratories)(26). Female *TgMISIIR-TAg* mice were generated by breeding male *TgMISIIR-TAg* mice to C57BL/6J females. Transgenic female offspring were monitored by baseline magnetic resonance imaging (MRI), as described ((27, 31) and below) to confirm the presence of ovarian tumor, defined as enlargement of one ovary to 50 mm^3, at which time mice were treated with vehicle (0.5% hypermellose/0.1%Tween 80) or AZD1480 (30 mg/kg in 0.5% hypermellose/0.1%Tween 80) by oral gavage (p.o.) twice daily (BID). Three separate cohorts of mice were randomized into two groups and treated as follows: For the *in vivo* drug efficacy study (cohort 1), mice (n=17/group) were treated with vehicle or AZD1480 on a 5 days on/2 days off schedule for 8-9 weeks, or until mice met humane criteria for euthanasia. For analysis of AZD1480 mediated alterations in gene expression (cohort 2), mice (n=4/group) with ∼500 mm^3 tumors were treated with vehicle or 30 mg/kg AZD1480 and euthanized 6 hours later for tumor tissue collection. For detection of tumor-associated protease activity (cohort 3), mice (n=5/group) were treated with vehicle or AZD1480 on a 5 days on/2 days off schedule for 3 weeks.

In vivo magnetic resonance imaging (MRI) and fluorescent molecular tomography (FMT)

Tumor growth was monitored and quantified by weekly imaging using a 7 Tesla vertical wide-bore magnet, equipped with a Bruker DRX 300 spectrometer as described (27, 31). The tumor volume was determined using three dimensional MRI data sets and volumetrics analysis to calculate tumor volume (27). Volumetric analysis was performed on datasets that were blinded with regard to treatment group. Weekly baseline images were initiated when mice were 8-10 weeks old. When the volume of one ovary reached 50 mm^3, drug or vehicle treatment was initiated. Once treatment commenced, mice were imaged weekly and the tumor volumes calculated. Tumor volume data were submitted to the biostatistician (S.L.) for analysis and determination of tumor growth rates. Prior work in our laboratory showed that ovarian tumors in *TgMISIIR-TAg* mice express integrin αvβ3 and activated tumor associated matrix metalloproteases MMPs that are predicted to contribute to tumor dissemination (31). To determine the effects of AZD1480 treatment on integrin αvβ3 expression and tumor-associated MMP activity, mice were subjected to FMT imaging for detection of the integrin αvβ3 binding imaging probe IntegriSense and activation of the MMP cleavable fluorescent imaging probe MMPSense as described (31). IntegriSense and MMPSense fluorescent imaging probes were purchased from Perkin Elmer. IntegriSense, is an integrin-targeted imaging agent that binds to integrin αvβ3 receptors and MMPSense is an optically silent molecular imaging probe that is activated in the presence of proteolytically active MMPs, including MMP2, 3, 7, 9, 12, and 13 (PerkinElmer, Inc). Tumor bearing mice (n=5/group) treated with vehicle or AZD1480 were given intravenous (retro-orbital) injections of MMPSense and IntegriSense (PerkinElmer, Inc) and subjected to combined FMT-MRI imaging as described (31).

Tissue preparation and analysis

Mice were euthanized, necropsied and examined for tumors and the presence of ascites (defined as the obvious presence of bloody, frequently cellular fluid upon midline incision through the abdominal wall). Reproductive tracts were removed and ovarian tumors length (l) and width (w) were measured with calipers and tumor volume calculated ($l \times w^2 \times 0.5$) (31). Individual portions of tumors were fixed in 10% neutral buffered formalin, paraffin embedded and sectioned for H&E staining and immunohistochemical detection of TAg as described (26). Additional portions of tumor tissue were snap-frozen in liquid nitrogen for protein analysis and RNA extraction. To evaluate immune cell populations in peritoneal washes, spleen and primary tumors, specimens were collected and processed at necropsy. Peritoneal cavities were washed with PBS supplemented with 2%FBS, spleens and portions of tumors were harvested. Spleens were dissociated between sterile glass slides; tumors were cut into small pieces and incubated in a dissociation mixture of (0.09% collagenase, 0.09% dispase, 0.9% FBS in DMEM). Red blood cells were removed incubation with 0.84% NH_4Cl. For staining of intracellular markers, cell samples were prepared with the BD Cytofix/Cytoperm™ Kit (BD Biosciences) according to manufacturer's instructions.

Flow Cytometry

Cells were isolated from peritoneal washes and from similar size spleen or primary tumor tissue and cell number was determined and normalized to ensure comparable analysis was

performed. Cells were preincubated with anti-Fc_{γ}III/IIR antibody (provided by L.J.S.) to block nonspecific binding and then stained with a mixture of fluorophore-labeled antibodies: CD45 eFlour450, CD19 PE, Foxp3 APC (eBioscience, Inc); F4/80 APC, CD11b PE, CD4 FITC, Ly-6G/Ly-6C (Gr-1) PE-Cy7 (BioLegend). Samples of cell suspensions were analyzed with a BD LSRII flow cytometer (BD Biosciences) and data were analyzed with FlowJo software (Tree Star Inc).

Microarray analysis and quantitative RT-PCR

Mouse tissue RNA samples were prepared using the RNeasy Mini Kit (QIAGEN) according to manufacturer's instructions and submitted to the Fox Chase Cancer Center (FCCC) Genomics Facility for gene expression analyses by microarray and quantitative RT-PCR. The RNA concentrations were determined with a NanoDrop spectrophotometer (Thermo Fisher Scientific) and quality was determined by Agilent Bioanalyzer RNA kits (Agilent) and the RNA integrity (RIN) numbers were between 9.5 and 10. RNA was subsequently amplified and labeled using the low RNA input linear amplification kit (Agilent) and labeled cRNA targets hybridized onto Agilent Mouse Whole Genome 4×44K microarrays. Raw expression data obtained from Agilent microarrays were background corrected and quantile normalized across experimental conditions (32). The LIMMA (Linear Models for Microarray Data) (33) methodology was applied to the log2-transformed expression data to identify differentially expressed genes across conditions. Gene Ontology (GO) enrichment analysis of the significant genes were done using GOstats package in Bioconductor (34). The LIMMA module in the Open Source R/Bioconductor package was utilized in the computations (34). Differentially expressed genes were identified based on statistical significance ($p<0.01$) as well as biological significance using fold change cutoff of 2. Five genes of interest then were validated by qRT-PCR using Taqman™ probes for *Ccdn1*, *Ccl12*, *Ifi204*, *Cd151*, *Stat3*, and *Rasd1* and three potential normalizer genes (35) *Ppib*, *Gusb* and *Hprt1* using the following assays from Life Technologies Mm01617100_m1 (*Ccl12*), Mm00432359_m1 (*Ccnd1*), Mm00492602_m1 (*Ifi204*), Mm00456961_m1 (*Stat3*), Mm00842185_g1 (*Rasd1*), Mm00446956_m1 (*Gusb*), Mm00446968_m1 (*Hprt1*) and Mm00478295_m1 (*Ppib*). RNA was DNAse treated with Turbo DNAse-free (Ambion) and reverse transcribed using Moloney murine leukemia virus reverse transcriptase (Ambion) and a mixture of anchored oligo-dT and random decamers. Two reverse-transcription (RT) reactions were performed for each sample using 100 or 25 ng of input RNA. For one vehicle-treated control used as calibrator, RT was also performed with 6.25, 1.56 and 0.39 ng of input RNA. PCR reactions were performed using an Applied Biosystems 7900 HT Instrument. Ct (cycle threshold) values were converted to quantities (in arbitrary units) using the standard curve established with the calibrator sample. The expression levels were normalized to *Ppib*. For each sample, the values are average and standard deviation of the data derived from two RT reactions.

Statistical analysis

Statistical analysis for all *in vitro* assays was conducted with Prism 5.0 (GraphPad Software). All imaging data (MRI and FMT) and endpoint analyses (tumor volume, presence or absence of ascites, flow cytometry data) were submitted to the Biostatistics and

Bioinformatics Facility for analysis. Specific analyses performed for each assessment are described in the results and figure legends. In all cases, $p<0.05$ were considered significant.

Results

In vitro effects of AZD1480 treatment on OC cell lines

Constitutive activation of STAT3 is common in ovarian carcinoma cell lines and tumors (7, 9, 10, 36, 37). While RNA-interference strategies can be used for *in vitro* studies, there are currently no STAT3-specific small molecule inhibitors that can be used for *in vivo* studies. As JAKs are key upstream mediators of STAT3 activation in solid tumors (16), we sought to determine the effects of targeted inhibition of JAKs on STAT3 activation in cell culture and mouse models of OC. To evaluate the effects of JAK/STAT3 pathway inhibition on viability, apoptosis and proliferation of OC cells, the small molecule inhibitor AZD1480 was chosen based on its potent JAK1/2-selective activity and inhibition of STAT3 signaling in several solid tumor models and have been used successfully in models of other solid tumors (6, 20-25). Exposure of human (A1847, OVCAR-5 and OVCAR-8) and murine (MOVCAR-5009 and MOVCAR-5447) OC cells to increasing concentrations of AZD1480 (0, 0.05, 0.1, 1, 5 and 10 μmol/L) for 24 hours resulted in dose dependent inhibition of STAT3 activation, measured by evaluating $pSTAT3^{Y705}$ levels by immunoblot analysis (Fig. 1A) and binding to a specific radiolabeled DNA element by EMSA (Supplemental Fig. SF1). Substantial reductions of $pSTAT3^{Y705}$ protein and DNA binding were observed at 0.05 or 0.1 μmol/L AZD1480, with little or no detectable levels remaining in cells treated with 1 μmol/L. Consistent with previous studies on cell lines from several solid tumors (6, 16, 20), low concentrations (0, 0.05, 0.1 and 1 μmol/L) of AZD1480 that significantly depleted $pSTAT3^{Y705}$ had no discernible effect on cell viability, although it was significantly reduced in the presence of 5 μmol/L AZD1480 (Fig. 1B and Supplementary Fig. S1A). In agreement, accumulation of annexin V^+ apoptotic cells was seen in the presence of 5.0 μmol/L AZD1480, with cleaved PARP levels observed at lower concentrations of drug (0.5-1.0 μmol/L; Fig. 1C). Similarly, cell proliferation was inhibited only in the presence of high concentration (5 μmol/L) AZD1480 (Fig. 1D). Similar results were observed in cultured murine ovarian carcinoma (MOVCAR) cells; AZD1480 treatment or inhibition of STAT3 by STAT3-targeting shRNA or the small molecule STATTIC, had little effect on cell viability or proliferation (Supplementary Fig. S1AB-D). Collectively, these results show that low doses of AZD1480 potently inhibited STAT3 activation in cultured OC cells without significantly affecting the viability or proliferative capacity of these cells. Although higher doses of AZD1480 induced significant apoptosis, these findings suggest that additional factor(s) besides direct induction of apoptosis in cultured OC cells (e.g., effects on the tumor microenvironment and/or cytokine or chemokine signaling) may contribute to the full effect of the drug *in vivo*.

We therefore sought to evaluate the effect on AZD on other aspects of OC cell biology in cultured cells. Dissemination of OC occurs primarily through local spread in the abdominal cavity, requiring the capacity of tumor cells to shed from the primary tumor, migrate and adhere to secondary sites in the peritoneum (38). Previous work showed that activated STAT3 is a key mediator of OC motility (7, 39); therefore, the effects of AZD1480 on cell

migration were evaluated using trans-well chemotactic migration assays. Migration was significantly reduced in A1847, OVCAR-5 and OVCAR-8 cells treated with 1 μmol/L AZD1480 (Fig. 1E). Similarly, pre-treatment with 1 μmol/L AZD1480 inhibited the capacity of A1847, OVCAR-5 and OVCAR-8 cells to adhere to fibronectin or type I collagen (Fig. 1F). Together, these results show that AZD1480 inhibits STAT3 activation and OC cell migration and adhesion, suggesting the potential for blockade of JAK/STAT3 signaling to inhibit OC growth and dissemination *in vivo*.

AZD1480 inhibits OC growth and ascites production in transgenic mice

We used a transgenic mouse model of OC to evaluate the therapeutic potential of AZD1480 *in vivo*. Transgenic MISIIR-TAg mice develop spontaneous OC that resembles high grade serous OC with 100% penetrance (26, 27). This model is particularly appropriate for this analysis, as full transformation by SV40 large TAg requires STAT3 (40) and tumors and cell lines derived from tumor bearing mice exhibit high levels of constitutively activated STAT3 (Fig. 1A and data not shown). Moreover, the presence of a functional immune system enables evaluation of the effects of JAK/STAT3 inhibition on the immune tumor microenvironment. To assess the impact of AZD1480 on tumor growth, mice were dosed twice daily with 30 mg/kg by oral gavage, based on previous studies (16, 20) and on pilot pharmacodynamic studies; in tumor bearing MISIIR-TAg mice, treatment with 30 mg/kg AZD1480 resulted in dramatically reduced $pSTAT3^{Y705}$ levels at 2 and 6 hours post treatment, with recovery at 24 hours (Supplementary Fig. S2). The presence of tumors in mice was confirmed by magnetic resonance imaging (MRI); once ovary volume reached $50mm^3$ (Fig. 2A-B) mice were randomized for treatment with AZD1480 or vehicle (n=17 mice/group). Mice were treated for 8-9 weeks, and tumor growth was monitored and quantified by weekly MRI. Longitudinal growth data demonstrated a highly significant ($p<0.0001$) delay in tumor growth rate and smaller ovarian tumors ($p<0.001$) in the AZD1480-treated mice compared to vehicle treated controls (Fig. 2C-D). Caliper measurements confirmed the tumor volumes calculated MRI data, showing significantly smaller tumors in AZD1480-treated mice (Fig. 2E and Fig. 3A). Moreover, significantly fewer mice had detectable ascites at necropsy; 2/17 (12%) AZD1480-treated mice compared to 12/17 (70%) vehicle-treated mice (Fig. 2F, $p=0.0013$). This study was designed to evaluate the effect of a limited period of AZD1480 treatment on the growth of radiologically confirmed, actively growing tumors. As such, the study did not address prevention of tumor formation or survival post drug withdrawal. In many cases, vehicle-treated mice met humane criteria for euthanasia prior to the study endpoint; on average, mice were vehicle-treated for 39 days and lived to 158 days. Most mice in the AZD1480 group remained on drug for the duration of the study (on average, AZD1480-treated 53 days), and lived to 181 days. Though the mice in the AZD1480 treated group lived longer ($p=0.014$), tumors grew while mice were on drug (compare Fig. 2B with C-E), suggesting tumors would continue to progress if drug were withdrawn.

To confirm AZD1480-mediated inhibition of STAT3 activation, snap frozen tumor tissue specimens were evaluated by immunoblot and ELISA for detection of $pSTAT3^{Y705}$ levels. Immunoblot analysis showed reduced $pSTAT3^{Y705}$ levels (Fig. 3B). An ELISA was used to quantify $pSTAT3^{Y705}$ levels, further validating the significant ($p<0.0001$) AZD1480-

mediated reduction of STAT3 activation in tumors (Fig. 3C). Taken together, these results show that AZD1480 results in significant tumor growth inhibition and that this effect may be due, at least in part, to reduction of STAT3 activity in primary tumors.

Gene expression is altered in tumors from AZD1480-treated mice

The primary functional consequences of STAT3 activation are related to its role as a transcription factor (41). To define the effects of AZD1480 treatment on STAT3-mediated transcription, RNA was isolated from ovarian tumors of mice that were treated with AZD1480 or vehicle (n=4/group) and global changes in gene expression were analyzed by genome wide microarray analysis (Geo accession number GSE63092: http://www.ncbi.nlm.nih.gov/geo/query/acc.cgi?acc=GSE63092). Unsupervised clustering analysis allowed separation into two groups; drug-treated tumors clustered separately from vehicle treated controls (data not shown). Using 2-fold change and $p<0.01$ cutoff we identified a list of 10 upregulated and 87 downregulated genes in AZD1480 treated tumors (Fig. 4A and Supplementary Table S1). Notably, the list of differentially expressed genes included a large number of genes previously shown to be regulated by STAT3 (42), including genes involved in cancer and wound healing and inflammation and immune response (e.g., *Ccnd1*, *Ccl12*, *Cepd*, *Ifiti1*, *Mx1*, *Mx2*, *Oas1*, *Oas2*, *Usp18*). Differentially expressed genes were found to be significantly enriched for ribonucleoside metabolic process and interferon and cytokine-mediated signaling pathways with Gene ontology (GO) enrichment analysis (Supplementary Table S2). A subset of genes was selected for individual validation by qRT-PCR. Differential expression was shown for *Ccdn1*, *Ccl12*, *Ifi204*, *Cd151*, *Stat3*, and *Rasd1* (Fig. 4B). These results confirm the direct inhibitory effects of AZD1480 on STAT3 transcriptional activity *in vivo*, and strongly suggest that the observed tumor growth inhibition result was due to inhibition of STAT3.

AZD1480 treatment inhibits tumor-associated integrin αvβ3 expression and MMP activity

Expression of integrin αvβ3 and activation of tumor-associated matrix metalloproteinases (MMPs) in tumor and stromal cells is an essential component of OC growth and dissemination (43-46). As MMP expression can be induced by activated STAT3 (42, 47-49), we hypothesized that the AZD1480-mediated tumor growth inhibitory effects were due in part to inhibition of tumor-associated integrin αvβ3 signaling and MMP activation. To investigate this directly, we used methods developed in our laboratory for combined anatomic and fluorescent molecular tomography (FMT) to detect and quantify *in vivo* integrin αvβ3 expression and MMP activation (31). Mice with ovarian tumors were treated with vehicle or AZD1480 (n=5/group) for four weeks and imaged weekly by MRI and FMT to determine tumor volume and to quantify integrin αvβ3 and MMP probe binding and activation. Once again, AZD1480 treated mice exhibited significantly reduced tumor growth as evidenced by MRI (Fig. 5A-B). In addition, there was a significant reduction in integrin αvβ3 probe binding and in MMP probe activation (Fig. 5A, C & D). These results confirm the *in vivo* tumor growth inhibitory effects of AZD1480 treatment and suggest that the tumor inhibitory effects of this agent are mediated in part by decreased tumor-associated integrin αvβ3 expression and MMP activity.

Effects of JAK/STAT3 inhibition on immune cell populations

The well-established feed-forward signaling between STAT3 in tumors and in the microenvironment (50, 51) and the lack of effect of AZD1480 treatment on cell growth, viability and survival in cultured OC cells, suggested that the tumor growth inhibitory effects of targeted disruption of the JAK/STAT3 pathway may not be confined to the activity of the drug only in tumor cells. Current thinking in OC research emphasizes the potential importance of targeting the pro-tumorigenic inflammatory response as an adjunct to conventional and tumor-targeted therapies (52). At the outset of this study, we hypothesized that targeted inhibition of JAK/STAT3 with AZD1480 would exert effects on both tumor cells and on immune cells in the tumor microenvironment, for example by inhibiting pro-tumorigenic, immunosuppressive tumor associated macrophages, myeloid derived suppressor cells (MDSC) or regulatory T (T_{reg}) cells. By employing an immunocompetent GEM model of OC, we were able to assess the effects of AZD1480 on immune cell populations in the spleen, tumors and in the peritoneal microenvironment, the principal site of OC dissemination. Immune cell populations were stained and analyzed by flow cytometry for detection of $CD45^+CD4^+$ T cells, $CD45^+F4/80^+CD11b^+$ macrophages, $CD45^+CD11b^+Gr\text{-}1^+$ MDSCs and $CD45^+CD4^+FoxP3^+$ T cells, in a subset of the original cohort of 34 mice evaluated for drug efficacy. Analysis of tumors showed that the number of infiltrating leukocytes was small, and that the majority of these cells were $CD45^+F4/80^+CD11b^+$ macrophages (Supplementary Fig. S3A). Notably, analysis of leukocyte populations present in the peritoneal cavity showed that while there were no significant differences in $CD45^+F4/80^+CD11b^+$ macrophages or $CD45^+CD11b^+GR\text{-}1^+$ MDSCs (Supplementary Fig. S3B) there was a significant reduction in both the number and percent of $CD45^+CD4^+$ and $CD45^+CD4^+FoxP3^+$ T cells in AZD1480-treated mice compared to controls (Fig. 6A-B). There were no significant differences in either of these populations detected in the spleens of vehicle- and drug-treated mice (Fig. 6A-B). These observations show that AZD1480-treatement is accompanied by reduction of pro-tumorigenic T cell subpopulations in the peritoneal cavity while splenic immune cell subpopulations remain unchanged.

Discussion

A significant majority of patients with advanced stage OC experience disease recurrence and eventually develop resistance to front-line chemotherapy. With the exception of anti-angiogenic therapies (e.g., bevacizumab) or poly-ADP-ribose polymerase (PARP) inhibitors, few promising agents have emerged for patients with recurrent and/or drug-resistant disease that meaningfully or durably extend survival. In cancers like OC that lack common, specific, drug-targetable oncogenic driver mutations (2), therapeutic targeting of proteins that have broad-spectrum pro-tumorigenic activities may be the most effective strategy. We have already explored this approach, showing that inhibition of heat shock protein 90 (HSP90) was highly effective in preclinical models of OC (3), and establishing a clinical trial to evaluate ganetespib, a small molecule HSP90 inhibitor, in combination with paclitaxel in OC in patients (NCT01962948). Like HSP90, the importance of persistent activation of STAT3 in a variety of human cancers, including OC, is well-established (5, 7, 9, 10). STAT3 activation may occur via multiple upstream signals, including activation via

IL-6/IL-6R-mediated activation of JAK2, which is a prominent mechanism present in OCs (11, 12). Activated growth factor receptor and non-growth factor tyrosine kinases (e.g., Src family kinases) may also play a role in STAT3 activation, with prior work suggesting that JAK family kinases may cooperate with these proteins to activate STAT3 (16). Constitutive STAT3 activation has tumor cell intrinsic consequences as well as effects within the extracellular matrix and stromal cells of the tumor microenvironment, resulting in increased tumor cell proliferation, survival, motility and invasiveness, as well as tumor-promoting angiogenesis and evasion of tumor suppressing immunity. While these broad ranging activities make STAT3 an attractive therapeutic target, druggability has been challenging due to the lack of intrinsic catalytic activity of the protein. In the absence of direct pharmacologic inhibitors of STAT3 that are suitable for *in vivo* use, an alternate strategy for inhibiting STAT3 function is to target direct upstream activators, or other mediators of its function and/or stability. Our prior work showed significant ganetespib-mediated inhibition of STAT3 activation in cultured OC cells and xenografts, and synergistic inhibition of OC cell viability when ganetespib was combined with a JAK inhibitor (3).

In this study, we investigated the potential efficacy of directly targeting JAK/STAT3 activation in OC using the small molecule JAK1/2 inhibitor AZD1480. Consistent with previous studies in other solid tumors (6, 16, 20), AZD1480 treatment resulted in significant inhibition of STAT3 phosphorylation ($pSTAT3^{Y705}$) and DNA binding at low drug concentrations; however, similar concentrations of drug had little effect on cell viability, proliferation or survival of cultured OC cells. It is now becoming clear that cytotoxic effects of JAK kinase inhibitors are largely limited to cells of hematological origin, particularly JAK-mutant MPN lines, and rarely seen in solid tumor cell lines in culture. The work describing AZD1480 (16) evaluated the effects of this compound and similarly showed low or no cytotoxicity in several cultured solid tumor cell lines, but tumor growth inhibition in xenografts. Similar observations of significant tumor growth inhibition of cell line xenografts that exhibited of low *in vitro* cytotoxicity have been made in several solid tumor models (6, 20-25, 53). The underlying reasons for these seemingly discordant results are unclear, but may be attributed to possible effects specific to conditions of 2D-cell culture or alternatively effects of the tumor microenvironment and/or disruption of a critical cytokine-mediated signaling axis, e.g., IL-6 (6, 21). The capacity of cells to migrate and adhere to type I collagen or fibronectin was also significantly reduced in cells treated with AZD1480. This finding is consistent with prior work demonstrating a direct role for STAT3 in mediating migration in cultured OC cells (7). Therefore, though AZD1480 exhibited low cytotoxicity in cultured OC cells it did suppress STAT3 activity via decreased phosphorylation and DNA binding, and by inhibiting STAT3-related functional properties required for OC dissemination. Maximal effects of JAK-targeted inhibition may require the complex interaction of the tumor microenvironment, which is supported by the ‘feed forward loop’ described in mammary and renal carcinomas and by the pro-tumorigenic effects of JAK/STAT3 signaling in immune cells in the tumor microenvironment (13-15).

In vivo, we showed significant inhibition of tumor growth rate, final tumor volume and production of malignant ascites in ovarian tumor-bearing transgenic mice treated with AZD1480 as a single agent. Tumor growth inhibition was accompanied by reduced levels of

pSTAT3^{Y705}, significant inhibition of tumor-associated MMP activity and altered gene expression in the AZD1480 treated mice. Many of the differentially expressed genes identified by microarray analysis are well-established STAT3 transcriptional targets (42). Direct AZD1480-mediated effects on tumor cell proliferation and survival are suggested by significant down-regulation of Cyclin D1 (*Ccnd1*), a key mediator of STAT3-induced proliferation, and up-regulation of *Rasd1*, a Ras-related protein associated with induction of apoptosis (10, 54). Expression and activation of tumor-associated MMPs and signaling through integrins is central to extracellular matrix remodeling and OC tumor progression in human OC and in MISIIR-TAg transgenic mice (31, 43-48). However, tumor-associated MMPs are largely produced by stromal cells, and detection of MMP protein levels by immunohistochemistry or immunoblot analyses does not provide information regarding tumor-associated protease activity (55). Using a combined FMT/MRI approach developed in our lab (31), we showed JAK inhibitor treatment resulted in significant inhibition of integrin αvβ3 probe binding and MMP probe activation, strongly supporting a central role for JAK/STAT3 in regulation of tumor-associated MMP activity. The significant reduction in ascites formation in AZD1480-treated mice may also be related to inhibition of tumor-associated MMPs in the tumor microenvironment.

Interestingly, analysis of differentially expressed genes in tumors from vehicle- and AZD1480-treated mice revealed subsets of genes related to interferon and cytokine responses as well as genes related to innate immune response, host defense and immune system processes. These changes strongly support the importance of JAK/STAT3 signaling in interactions of tumor cells and tumor-associated inflammation in OC development. Prior work demonstrated alterations in infiltrating immune cell populations in immune competent mouse models of mammary carcinoma (6). Specifically, mice treated with AZD1480 exhibited significant reduction of tumor infiltrating $CD45^+CD11b^+Gr\text{-}1^+$ myeloid derived suppressor cells. In our analysis of infiltrating immune cells present in tumors and the peritoneal tumor microenvironment showed no significant differences in the number or percent of immunosuppressive $CD45^+CD11b^+Gr\text{-}1^+$ MDSCs or $CD45^+F4/80^+CD11b^+$ macrophages. The reasons for the lack of effect on MDSCs are unclear, but suggest that the effects of JAK inhibitors may be tissue-specific. Interestingly, there was a significant reduction in both $CD45^+CD4^+$ T cells and $CD45^+CD4^+Foxp3^+$ T cells present in the peritoneal tumor microenvironment. It is possible that the reduction in $Foxp3^+$ cells may be a reflection of the reduction in total number of $CD45^+CD4^+$ cells, but this appears not to be a general effect of the drug, as there is no difference in these sub-populations in the spleens of drug- or vehicle-treated mice. The reduction of $CD45^+CD4^+Foxp3^+$ cells is noteworthy, as T_{reg} cells are key mediators of immune suppression and angiogenesis, and the presence of high levels of T_{reg} cells is inversely correlated with survival in patients with OC (56, 57). The significant depletion of $CD45^+CD4^+Foxp3^+$ cells in the peritoneal tumor microenvironment of AZD1480-treated mice suggests that tumor growth inhibition is mediated, at least in part, by effects of the drug on tumor-associated immunosuppressive inflammatory cells. Unlike the inhibition of T_{reg} cells in the peritoneal cavity, we observed relatively low number of tumor infiltrating leukocytes in primary tumors from vehicle or drug-treated mice. Therefore, while AZD1480-mediated inhibition may block ascites formation via effects on pro-tumorigenic inflammation, primary tumor growth may be

affected to a lesser extent by drug-mediated effects on inflammation. While AZD1480 exhibited little toxicity in monolayer cultured cells, we cannot rule out the possibilities it may inhibit growth or survival cells in tumors *in vivo*, or may influence other elements of the microenvironment including the pro-tumorigenic activities of tumor-associated fibroblasts or angiogenesis, or cytokine and/or chemokine signaling networks (6, 21).

Further studies of the effects of targeted inhibition of JAK/STAT3 inhibition on T_{reg} cell production and function are warranted, as these cells are believed to be central to OC tumor development and progression and depletion of these cells has been proposed as a therapeutic strategy for treatment of OC patients.

Consistent with observations in preclinical models of other solid tumors (6, 16, 21, 24, 25) our data show that targeted inhibition of the JAK/STAT3 pathway with AZD1480 significantly inhibits ovarian tumor growth in a transgenic mouse model of OC. Our data suggest that the pharmacologic inhibition of JAK1/2 with AZD1480 has direct effects on tumor cells as well as tumor-associated MMPs in the ECM and infiltrating immune cells in the peritoneal microenvironment. However, the absence of tumor regression suggests that the most effective strategy for incorporation of JAK/STAT3 pathway inhibitors will be by identifying combination therapies that maximize anti-tumor response. A recent study investigating the combination of a JAK inhibitor (ruxolitinib) and cisplatin in NSCLC showed the combination was additive or antagonistic in cisplatin sensitive cells with low JAK2 expression, but synergistic or strongly synergistic in cisplatin-resistant cells with high JAK2 levels (58). This suggests that combination of a JAK/STAT3 inhibitor with platinum therapy may be effective, particularly in cancers with high levels of JAK/STAT3 activation. The significant and broad effects of JAK/STAT3 pathway inhibition support further investigation of this class of inhibitors in combination with standard cytotoxic agents or other targeted therapeutics for treatment of OC.

Supplementary Material

Refer to Web version on PubMed Central for supplementary material.

Acknowledgments

We gratefully acknowledge Dr. Glenn Rall for helpful discussions and critical review of this manuscript. We thank Ms. Ellen Neulight for assistance with genotyping transgenic mice. This work was supported by the FCCC Laboratory Animal, High Throughput Screening, Cell Culture, Biosample Repository, Biomedical Imaging, Histopathology and Biostatistics and Bioinformatics Facilities.

Grant Support: This work was supported, in part, by a grant with the Pennsylvania Department of Health. The Department specifically disclaims responsibility for any analyses, interpretations or conclusions. This work was also supported by R01 CA136596 (to D.C. Connolly) and the FCCC Comprehensive Cancer Center Core Grant NCI P30 CA006927 (to R.I. Fisher). This work was also supported by charitable donations from the Teal Tea Foundation and the Bucks County Board of Associates (to D.C. Connolly).

Financial Support: This project was funded, in part, by an award from a grant with the Pennsylvania Department of Health (SAP#4100054848) to D.C. Connolly. The Department specifically disclaims responsibility for any analyses, interpretations or conclusions. This work was also supported by R01 CA136596 (to D.C. Connolly), the FCCC Comprehensive Cancer Center Core Grant NCI P30 CA006927 (to Principal Investigator R.I. Fisher) and by charitable donations from the Teal Tea Foundation and the Bucks County Board of Associates (to D.C. Connolly).

References

1. Siegel R, Ma J, Zou Z, Jemal A. Cancer statistics, 2014. CA Cancer J Clin. 2014; 64:9–29. [PubMed: 24399786]
2. TCGA. Integrated genomic analyses of ovarian carcinoma. Nature. 2011; 474:609–15. [PubMed: 21720365]
3. Liu H, Xiao F, Serebriiskii IG, O'Brien SW, Maglaty MA, Astsaturov I, et al. Network analysis identifies an HSP90-central hub susceptible in ovarian cancer. Clin Cancer Res. 2013; 19:5053–67. [PubMed: 23900136]
4. Gao SP, Bromberg JF. Touched and moved by STAT3. Sci STKE. 2006; 2006:pe30. [PubMed: 16835434]
5. Avalle L, Pensa S, Regis G, Novelli F, Poli V. STAT1 and STAT3 in tumorigenesis: A matter of balance. JAKSTAT. 2012; 1:65–72. [PubMed: 24058752]
6. Chang Q, Bournazou E, Sansone P, Berishaj M, Gao SP, Daly L, et al. The IL-6/JAK/Stat3 feed-forward loop drives tumorigenesis and metastasis. Neoplasia. 2013; 15:848–62. [PubMed: 23814496]
7. Silver DL, Naora H, Liu J, Cheng W, Montell DJ. Activated signal transducer and activator of transcription (STAT) 3: localization in focal adhesions and function in ovarian cancer cell motility. Cancer Res. 2004; 64:3550–8. [PubMed: 15150111]
8. Akira S. Roles of STAT3 defined by tissue-specific gene targeting. Oncogene. 2000; 19:2607–11. [PubMed: 10851059]
9. Duan Z, Foster R, Bell DA, Mahoney J, Wolak K, Vaidya A, et al. Signal transducers and activators of transcription 3 pathway activation in drug-resistant ovarian cancer. Clin Cancer Res. 2006; 12:5055–63. [PubMed: 16951221]
10. Huang M, Page C, Reynolds RK, Lin J. Constitutive activation of stat 3 oncogene product in human ovarian carcinoma cells. Gynecol Oncol. 2000; 79:67–73. [PubMed: 11006034]
11. Kryczek I, Grybos M, Karabon L, Klimczak A, Lange A. IL-6 production in ovarian carcinoma is associated with histiotype and biological characteristics of the tumour and influences local immunity. Br J Cancer. 2000; 82:621–8. [PubMed: 10682675]
12. Nilsson MB, Langley RR, Fidler IJ. Interleukin-6, secreted by human ovarian carcinoma cells, is a potent proangiogenic cytokine. Cancer Res. 2005; 65:10794–800. [PubMed: 16322225]
13. Bollrath J, Phesse TJ, von Burstin VA, Putoczki T, Bennecke M, Bateman T, et al. gp130-mediated Stat3 activation in enterocytes regulates cell survival and cell-cycle progression during colitis-associated tumorigenesis. Cancer Cell. 2009; 15:91–102. [PubMed: 19185844]
14. Grivennikov S, Karin E, Terzic J, Mucida D, Yu GY, Vallabhapurapu S, et al. IL-6 and Stat3 are required for survival of intestinal epithelial cells and development of colitis-associated cancer. Cancer Cell. 2009; 15:103–13. [PubMed: 19185845]
15. Kortylewski M, Swiderski P, Herrmann A, Wang L, Kowolik C, Kujawski M, et al. In vivo delivery of siRNA to immune cells by conjugation to a TLR9 agonist enhances antitumor immune responses. Nat Biotechnol. 2009; 27:925–32. [PubMed: 19749770]
16. Hedvat M, Huszar D, Herrmann A, Gozgit JM, Schroeder A, Sheehy A, et al. The JAK2 inhibitor AZD1480 potently blocks Stat3 signaling and oncogenesis in solid tumors. Cancer Cell. 2009; 16:487–97. [PubMed: 19962667]
17. Kortylewski M, Kujawski M, Wang T, Wei S, Zhang S, Pilon-Thomas S, et al. Inhibiting Stat3 signaling in the hematopoietic system elicits multicomponent antitumor immunity. Nat Med. 2005; 11:1314–21. [PubMed: 16288283]
18. Yue P, Turkson J. Targeting STAT3 in cancer: how successful are we? Expert Opin Investig Drugs. 2009; 18:45–56.
19. Sen M, Thomas SM, Kim S, Yeh JI, Ferris RL, Johnson JT, et al. First-in-human trial of a STAT3 decoy oligonucleotide in head and neck tumors: implications for cancer therapy. Cancer Discov. 2012; 2:694–705. [PubMed: 22719020]
20. Xin H, Herrmann A, Reckamp K, Zhang W, Pal S, Hedvat M, et al. Antiangiogenic and antimetastatic activity of JAK inhibitor AZD1480. Cancer Res. 2011; 71:6601–10. [PubMed: 21920898]

21. Gu L, Talati P, Vogiatzi P, Romero-Weaver AL, Abdulghani J, Liao Z, et al. Pharmacologic suppression of JAK1/2 by JAK1/2 inhibitor AZD1480 potently inhibits IL-6-induced experimental prostate cancer metastases formation. Mol Cancer Ther. 2014; 13:1246–58. [PubMed: 24577942]
22. Katsha A, Arras J, Soutto M, Belkhiri A, El-Rifai W. AURKA regulates JAK2-STAT3 activity in human gastric and esophageal cancers. Mol Oncol. 2014; 8:1419–28. [PubMed: 24953013]
23. Lee JH, Park KS, Alberobello AT, Kallakury B, Weng MT, Wang Y, et al. The Janus kinases inhibitor AZD1480 attenuates growth of small cell lung cancers in vitro and in vivo. Clin Cancer Res. 2013; 19:6777–86. [PubMed: 24158701]
24. McFarland BC, Ma JY, Langford CP, Gillespie GY, Yu H, Zheng Y, et al. Therapeutic potential of AZD1480 for the treatment of human glioblastoma. Mol Cancer Ther. 2011; 10:2384–93. [PubMed: 22027691]
25. Stuart E, Buchert M, Putoczki T, Thiem S, Farid R, Elzer J, et al. Therapeutic inhibition of Jak activity inhibits progression of gastrointestinal tumors in mice. Mol Cancer Ther. 2014; 13:468–74. [PubMed: 24398427]
26. Connolly DC, Bao R, Nikitin AY, Stephens KC, Poole TW, Hua X, Harris SS, Vanderhyden BC, Hamilton TC. Female mice chimeric for expression of the SV40 TAg under control of the MISIIR promoter develop epithelial ovarian cancer. Cancer Research. 2003; 63:1389–97. [PubMed: 12649204]
27. Hensley H, Quinn BA, Wolf RL, Litwin SL, Mabuchi S, Williams SJ, et al. Magnetic Resonance Imaging for Detection and Determination of Tumor Volume in a Genetically Engineered Mouse Model of Ovarian Cancer. Cancer Biol Ther. 2007; 6
28. Connolly DC, Hensley HH. Xenograft and Transgenic Mouse Models of Epithelial Ovarian Cancer and Non Invasive Imaging Modalities to Monitor Ovarian Tumor Growth In situ -Applications in Evaluating Novel Therapeutic Agents. Current protocols in pharmacology / editorial board, SJ Enna. 2009; 45:14 2 1–2 26.
29. Do TV, Xiao F, Bickel LE, Klein-Szanto AJ, Pathak HB, Hua X, et al. Aurora kinase A mediates epithelial ovarian cancer cell migration and adhesion. Oncogene. 2014; 33:539–49. [PubMed: 23334327]
30. Thapa RJ, Basagoudanavar SH, Nogusa S, Irrinki K, Mallilankaraman K, Slifker MJ, et al. NF-kappaB protects cells from gamma interferon-induced RIP1-dependent necroptosis. Mol Cell Biol. 2011; 31:2934–46. [PubMed: 21576359]
31. Hensley HH, Roder NA, O'Brien SW, Bickel LE, Xiao F, Litwin S, et al. Combined in vivo molecular and anatomic imaging for detection of ovarian carcinoma-associated protease activity and integrin expression in mice. Neoplasia. 2012; 14:451–62. [PubMed: 22787427]
32. Bolstad BM, Irizarry RA, Åstrand M, Speed TP. A comparison of normalization methods for high density oligonucleotide array data based on variance and bias. Bioinformatics. 2003; 19:185–93. [PubMed: 12538238]
33. Smyth GK. Linear models and empirical bayes methods for assessing differential expression in microarray experiments. Stat Appl Genet Mol Biol. 2004; 3 Article3.
34. Gentleman RC, Carey VJ, Bates DM, Bolstad B, Dettling M, Dudoit S, et al. Bioconductor: open software development for computational biology and bioinformatics. Genome Biol. 2004; 5:R80. [PubMed: 15461798]
35. Johnson, G.; Nour, A.; Nolan, T.; Huggett, J.; Bustin, S. Minimum Information Necessary for Quantitative Real-Time PCR Experiments. In: Biassoni, R.; Raso, A., editors. Quantitative Real-Time PCR. Springer; New York: 2014. p. 5-17.
36. Burke WM, Jin X, Lin HJ, Huang M, Liu R, Reynolds RK, et al. Inhibition of constitutively active Stat3 suppresses growth of human ovarian and breast cancer cells. Oncogene. 2001; 20:7925–34. [PubMed: 11753675]
37. Savarese TM, Campbell CL, McQuain C, Mitchell K, Guardiani R, Quesenberry PJ, et al. Coexpression of oncostatin M and its receptors and evidence for STAT3 activation in human ovarian carcinomas. Cytokine. 2002; 17:324–34. [PubMed: 12061840]
38. Tan DS, Agarwal R, Kaye SB. Mechanisms of transcoelomic metastasis in ovarian cancer. The lancet oncology. 2006; 7:925–34. [PubMed: 17081918]

39. Colomiere M, Ward AC, Riley C, Trenerry MK, Cameron-Smith D, Findlay J, et al. Cross talk of signals between EGFR and IL-6R through JAK2/STAT3 mediate epithelial-mesenchymal transition in ovarian carcinomas. Br J Cancer. 2009; 100:134–44. [PubMed: 19088723]
40. Vultur A, Arulanandam R, Turkson J, Niu G, Jove R, Raptis L. Stat3 is required for full neoplastic transformation by the Simian Virus 40 large tumor antigen. Mol Biol Cell. 2005; 16:3832–46. [PubMed: 15917293]
41. Bromberg JF, Wrzeszczynska MH, Devgan G, Zhao Y, Pestell RG, Albanese C, et al. Stat3 as an Oncogene. Cell. 1999; 98:295–303. [PubMed: 10458605]
42. Dauer DJ, Ferraro B, Song L, Yu B, Mora L, Buettner R, et al. Stat3 regulates genes common to both wound healing and cancer. Oncogene. 2005; 24:3397–408. [PubMed: 15735721]
43. Beck V, Herold H, Benge A, Luber B, Hutzler P, Tschesche H, et al. ADAM15 decreases integrin alphavbeta3/vitronectin-mediated ovarian cancer cell adhesion and motility in an RGD-dependent fashion. Int J Biochem Cell Biol. 2005; 37:590–603. [PubMed: 15618016]
44. Landen CN, Kim TJ, Lin YG, Merritt WM, Kamat AA, Han LY, et al. Tumor-selective response to antibody-mediated targeting of alphavbeta3 integrin in ovarian cancer. Neoplasia. 2008; 10:1259–67. [PubMed: 18953435]
45. Leroy-Dudal J, Demeilliers C, Gallet O, Pauthe E, Dutoit S, Agniel R, et al. Transmigration of human ovarian adenocarcinoma cells through endothelial extracellular matrix involves alphav integrins and the participation of MMP2. Int J Cancer. 2005; 114:531–43. [PubMed: 15609323]
46. Schmalfeldt B, Prechtel D, Harting K, Spathe K, Rutke S, Konik E, et al. Increased expression of matrix metalloproteinases (MMP)-2, MMP-9, and the urokinase-type plasminogen activator is associated with progression from benign to advanced ovarian cancer. Clin Cancer Res. 2001; 7:2396–404. [PubMed: 11489818]
47. Landen CN, Lin YG, Armaiz Pena GN, Das PD, Arevalo JM, Kamat AA, et al. Neuroendocrine Modulation of Signal Transducer and Activator of Transcription-3 in Ovarian Cancer. Cancer Research. 2007; 67:10389–96. [PubMed: 17974982]
48. Seo JM, Park S, Kim JH. Leukotriene B4 Receptor-2 Promotes Invasiveness and Metastasis of Ovarian Cancer Cells through Signal Transducer and Activator of Transcription 3 (STAT3)-dependent Up-regulation of Matrix Metalloproteinase 2. Journal of Biological Chemistry. 2012; 287:13840–9. [PubMed: 22396544]
49. Xie, Tx; Wei, D.; Liu, M.; Gao, AC.; Ali-Osman, F.; Sawaya, R., et al. Stat3 activation regulates the expression of matrix metalloproteinase-2 and tumor invasion and metastasis. Oncogene. 2004; 23:3550–60. [PubMed: 15116091]
50. Yu H, Kortylewski M, Pardoll D. Crosstalk between cancer and immune cells: role of STAT3 in the tumour microenvironment. Nat Rev Immunol. 2007; 7:41–51. [PubMed: 17186030]
51. Yu H, Pardoll D, Jove R. STATs in cancer inflammation and immunity: a leading role for STAT3. Nat Rev Cancer. 2009; 9:798–809. [PubMed: 19851315]
52. Vaughan S, Coward JI, Bast RC Jr, Berchuck A, Berek JS, Brenton JD, et al. Rethinking ovarian cancer: recommendations for improving outcomes. Nat Rev Cancer. 2011; 11:719–25. [PubMed: 21941283]
53. Wen W, Liang W, Wu J, Kowolik CM, Buettner R, Scuto A, et al. Targeting JAK1/STAT3 Signaling Suppresses Tumor Progression and Metastasis in a Peritoneal Model of Human Ovarian Cancer. Mol Cancer Ther. 2014
54. Vaidyanathan G, Cismowski MJ, Wang G, Vincent TS, Brown KD, Lanier SM. The Ras-related protein AGS1/RASD1 suppresses cell growth. Oncogene. 2004; 23:5858–63. [PubMed: 15184869]
55. Davidson B, Trope CG, Reich R. The role of the tumor stroma in ovarian cancer. Front Oncol. 2014; 4:104. [PubMed: 24860785]
56. Curiel TJ, Coukos G, Zou L, Alvarez X, Cheng P, Mottram P, et al. Specific recruitment of regulatory T cells in ovarian carcinoma fosters immune privilege and predicts reduced survival. Nat Med. 2004; 10:942–9. [PubMed: 15322536]
57. Facciabene A, Motz GT, Coukos G. T-regulatory cells: key players in tumor immune escape and angiogenesis. Cancer Res. 2012; 72:2162–71. [PubMed: 22549946]

58. Harada D, Takigawa N, Kiura K. The Role of STAT3 in Non-Small Cell Lung Cancer. Cancers (Basel). 2014; 6:708–22. [PubMed: 24675568]

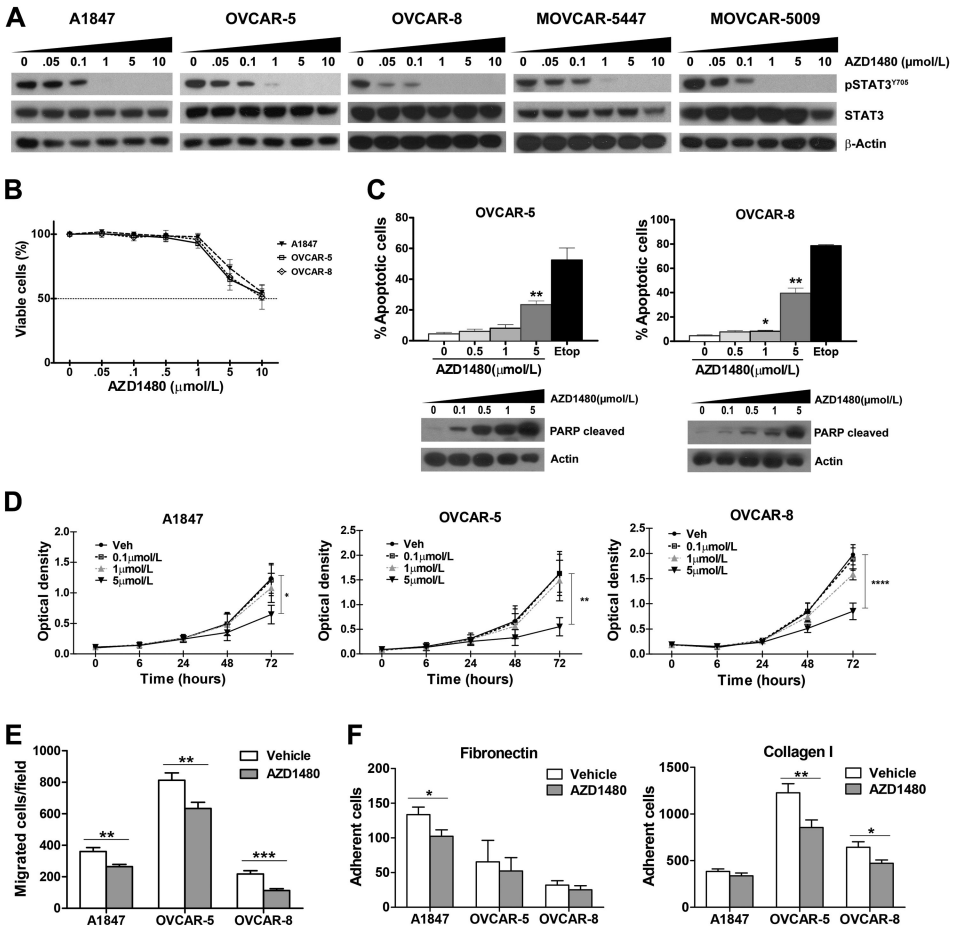

Figure 1. AZD1480 treatment reduces phosphorylated STAT3 levels and inhibits ovarian carcinoma cell migration and adhesion

A) Human (A1847, OVCAR-5 and OVCAR-8) and murine (MOVCAR-5447 and MOVCAR-5009) ovarian carcinoma cells were treated with DMSO (vehicle) or increasing concentrations AZD1480 (0.05, 0.1, 1, 5, 10 μmol/L) for 24 h and protein lysates subjected to immunoblot analysis with antibodies recognizing $pSTAT3^{Y705}$ and total STAT3. **B)** A1847, OVCAR-5 and OVCAR-8 cells were grown in the presence of DMSO (vehicle) or increasing concentrations AZD1480 (0.05, 0.1, 0.5, 1, 5, 10 μmol/L) for 72 hours and cell viability was determined by CellTiter Blue Viability Assay. Data indicate the mean percentage viability calculated from triplicate samples from 3 independent experiments (±SEM). **C)** OVCAR-5 and OVCAR-8 cells were treated with 0, 0.5, 1 or 5 μmol/L AZD1480 for 48 hours and analyzed for the presence of Annexin V-PE+ cells and PARP cleavage. Data shown are the mean values (± SEM) from three independent experiments. Cleaved PARP levels were detected by immunoblot analysis. **D)** The effect of increasing concentrations of AZD1480 on cell proliferation was determined by exposure of A1847, OVCAR-5 and OVCAR-8 cells to 0, 0.5, 1 or 5 μmol/L AZD1480 for 6, 24, 48 and 72 hours. Cells were fixed and stained with crystal violet, and plates read on a spectrophotometer to determine the optical density ($OD_{590\ nm}$). Data are presented as the mean $OD_{590\ nm}$ ±SEM (n=3). **E)** Chemotactic migration assays were performed to

determine the effects of 1.0 μmol/L AZD1480 treatment on migration of A1847, OVCAR-5 and OVCAR-8 cells. **F)** The effects of 1.0 μmol/L AZD1480 treatment on OC cell adhesion to fibronectin and type I collagen was determined. The bars depict the mean number of migrated or adherent cells ±SEM (n=3). Statistical analysis for data collected from viability and apoptosis assays was performed using one-way ANOVA test followed by multiple comparison test; proliferation assay data were analyzed with two-way ANOVA followed by multiple comparison test, migration and adhesion data were analyzed with unpaired t test. *P* values less <0.05 were considered significant (*p<0.05, **p<0.01, ***p <0.001, ****p<0.0001).

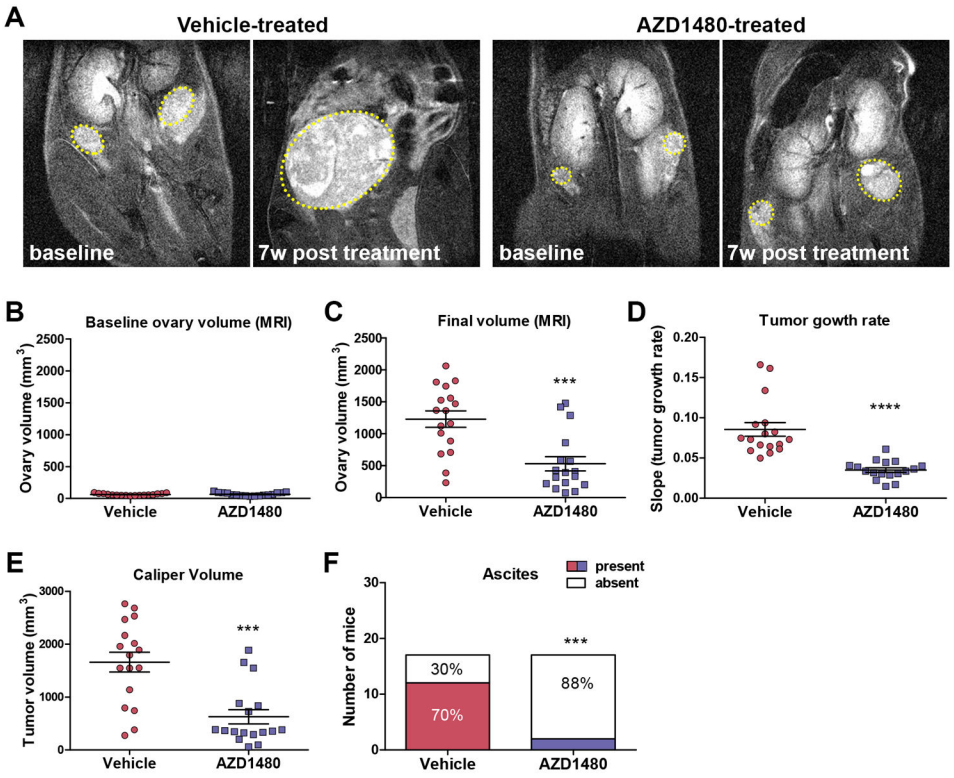

Figure 2. AZD1480-treatment inhibits ovarian tumor growth and ascites production in MISIIR-TAg mice

Spontaneous tumor development and growth in MISIIR-TAg mice was monitored by weekly magnetic resonance imaging (MRI) and drug treatment initiated when tumor volume reached ~50 mm^3. Equal numbers (n=17 mice/group) of MISIIR-TAg mice were treated with vehicle or 30 mg/kg AZD1480. **(A)** Representative images of MRI scans at baseline and after 7 weeks of treatment. Ovarian tumors are outlined in yellow dashed lines. Tumor volume calculated from MRI data for all mice at baseline (**B)** and final scans **(C)** prior to euthanasia. **D)** Weekly MRI datasets were subjected volumetrics analysis and slopes of log-transformed tumor growth rate calculated for each mouse. At necropsy, final tumor volume was determined by caliper measurements (**E)** and the presence or absence of malignant ascites was determined **(F)**. The MRI data for tumor growth rate were analyzed by the Wilcoxon signed-rank test, final tumor volumes by the Mann-Whitney t test and ascites fraction by the Fisher's exact two-sided test. *P* values less <0.05 were considered significant (***p <0.001, ****p<0.0001).

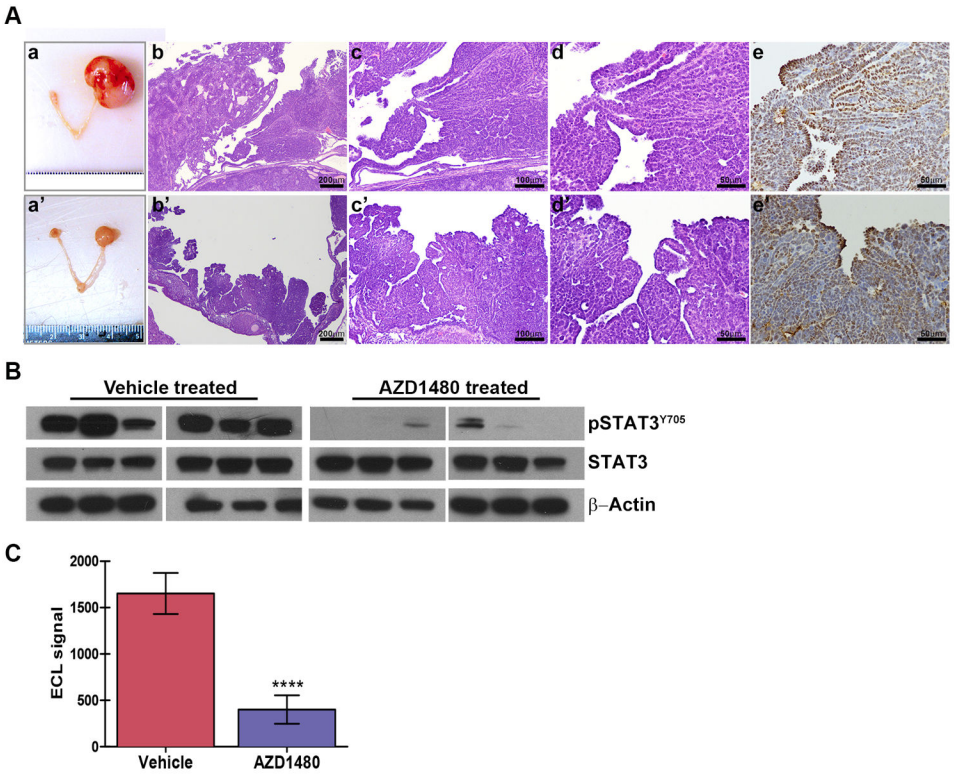

Figure 3. AZD1480-mediated tumor growth inhibition is accompanied by reduced STAT3 activation

(A) Gross images of reproductive tracts and light microscopic images of hematoxylin and eosin (H&E) and TAg stained sections of tumors from representative vehicle- (upper panels) or AZD1480-treated (lower panels) mice. Tumor tissue specimens from vehicle- and AZD1480-treated mice were harvested 6 hours after the last drug dose and analyzed by immunoblot **(B)** and electro chemiluminescent ELISA analysis **(C)** for detection and quantification of activating STAT3 phosphorylation at tyrosine 705 (pSTAT3^{Y705}). ****p<0.0001.

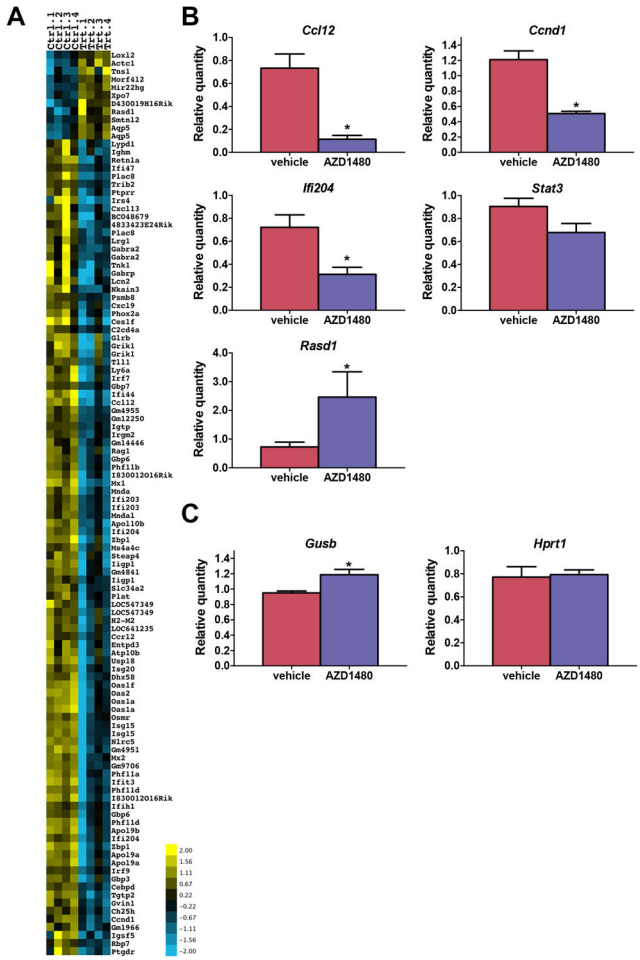

Figure 4. Expression of STAT3 target genes is altered in AZD1480-treated ovarian tumors

TgMISIIR-TAg mice with ~500 mm^3 ovarian tumors were treated with vehicle or 30 mg/kg AZD1480 (n=4 mice/group) and tumors were harvested 6 hours after drug treatment. RNA was isolated from tumors and analyzed by genome wide microarray analysis determine the effects of drug treatment on gene transcription. **A)** Heat map showing 10 upregulated and 87 downregulated genes (2-fold change and $p<0.01$ cutoff) in AZD1480-treated tumors. **B)** qRT-PCR validation differential expression of selected genes. **C)** qRT-PCR amplification of potenitial normalizing genes *Gusb* and *Hprt1*. Quantity was normalized to *Ppib*. (Error bars indicate ±SEM; data was analyzed using the Mann-Whitney t test, *$p<0.05$).

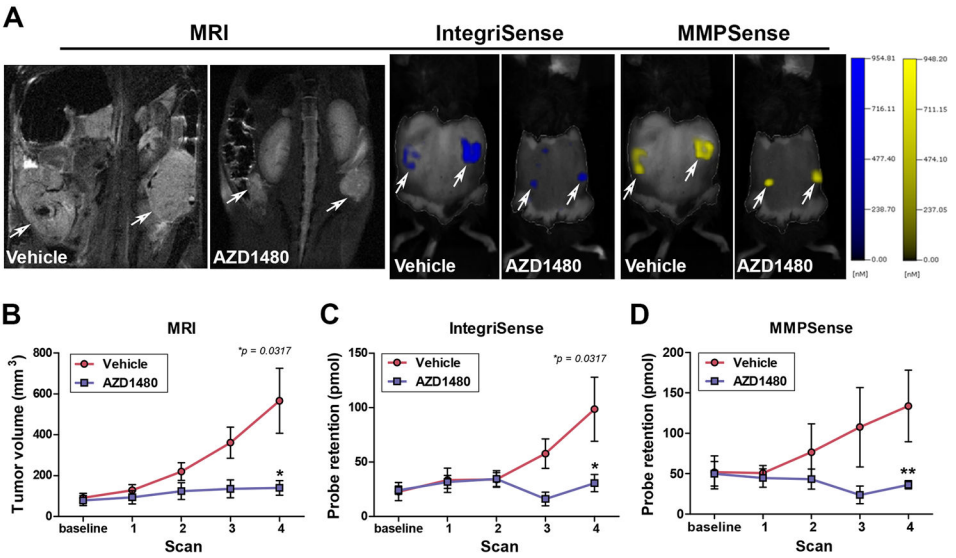

Figure 5. AZD1480 inhibits tumor-associated integrin αvβ3 expression and MMP activity

The tumor associated integrin αvβ3 expression and MMP activity was detected by combined anatomic imaging (MRI) and fluorescent molecular tomography (FMT). Tumor-bearing mice were treated with vehicle or AZD1480 (n=5/group) for 4 weeks and imaged weekly by MRI to monitor tumor growth and FMT to monitor integrin αvβ3 probe binding and MMP probe activation. **A)** Representative MRI images, IntegriSense probe binding and MMPSense probe activation in ovarian tumors in vehicle- and AZD1480-treated mice. Quantification of tumor volume by MRI **(B),** and IntegriSense probe retention **(C)** and MMP probe activation **(D)** by FMT. (**p*<0.05, ***p*<0.01).

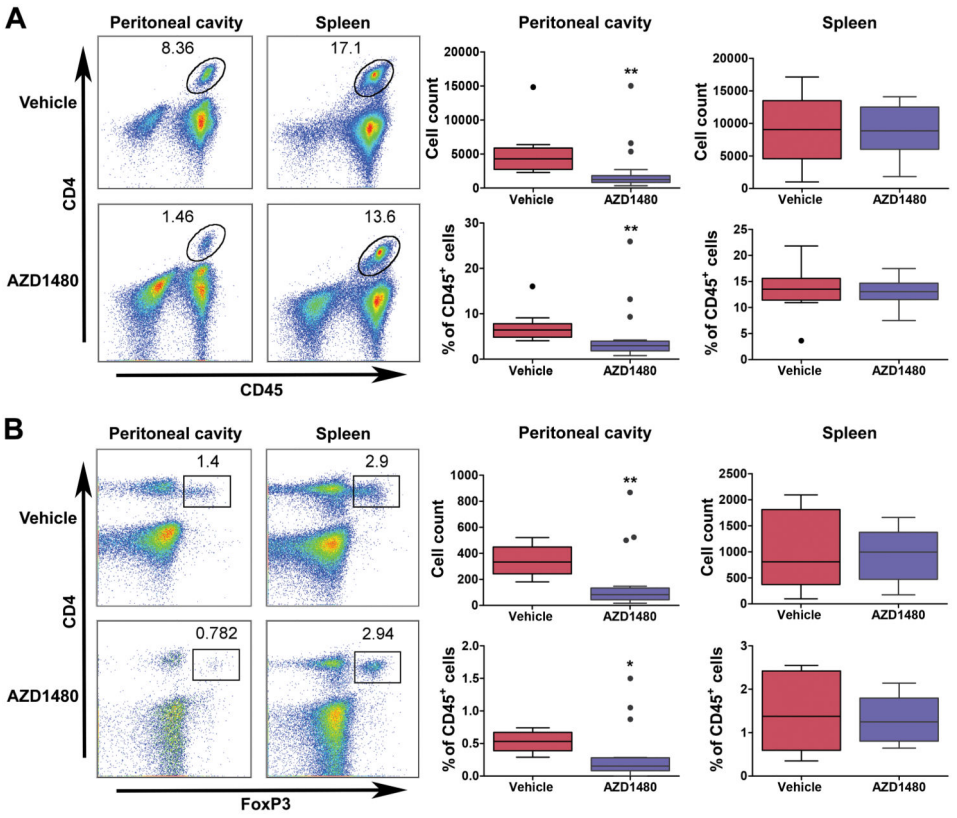

Figure 6. AZD1480-mediated JAK/STAT3 inhibition reduces T cell populations in the peritoneal tumor microenvironment

Cell suspensions were prepared from peritoneal washes and spleens harvested from vehicle- (n=12) and AZD1480-treated (n=19) mice and analyzed by flow cytometry. **A)** Representative flow cytometry dot plots and pooled data showing the number and percent (normalized to $CD45^+$ leukocytes) of $CD45^+CD4^+$ T cells in peritoneal cavity and spleen. **B)** Representative flow cytometry dot plots and pooled data showing the absolute number and percent (normalized to $CD45^+$ leukocytes) of $CD45^+CD4^+FoxP3^+$ T cells in peritoneal cavity and spleen. Bars show mean ±SEM (Vehicle: n=10; AZD1480: n =19). Statistical analysis is based on Wilcoxon test, *p<0.05, ** p <0.01.